

# Demonstration of an iodine laser pumped by an air-helium electric discharge

B. S. Woodard, J. W. Zimmerman, G. F. Benavides, D. L. Carroll\*, J. T. Verdeyen,  
A. D. Palla, T. H. Field  
CU Aerospace, 2100 S. Oak St. – Suite 206, Champaign, IL 61820  
W. C. Solomon  
University of Illinois, 306 Talbot Laboratory, 104 S. Wright St., Urbana, IL 61801  
S. Lee, W. T. Rawlins, S. J. Davis  
Physical Sciences Inc., 20 New England Business Center, Andover, MA 01810

## ABSTRACT

Herein the authors report on the demonstration of gain and a continuous-wave laser on the 1315 nm transition of atomic iodine using the energy transferred to  $I(^2P_{1/2})$  from  $O_2(a^1\Delta)$  produced by both radio-frequency and microwave electric discharges sustained in a dry air-He-NO gas mixture. Active oxygen and nitrogen species were observed downstream of the discharge region. Downstream of the discharge, cold gas injection was employed to raise the gas density and lower the temperature of the continuous gas flow. Gain of 0.0062 %/cm was obtained and the laser output power was 32 mW in a supersonic flow cavity.

**Keywords:** electric oxygen iodine laser, electric discharge, singlet oxygen, active nitrogen

## 1. INTRODUCTION

The classical chemical oxygen-iodine laser (COIL) reported by McDermott *et al.*<sup>1</sup> operates on the electronic transition of the iodine atom at 1315 nm,  $I(^2P_{1/2}) \rightarrow I(^2P_{3/2})$  [denoted hereafter as  $I^*$  and I respectively]. The lasing state  $I^*$  is produced by near resonant energy transfer with the singlet oxygen metastable  $O_2(a^1\Delta)$  [denoted hereafter as  $O_2(a)$ ]. The conventional COIL requires a chemical two-phase process to produce the  $O_2(a)$  from aqueous basic hydrogen peroxide and  $Cl_2$  gas. Logistic issues with this chemical singlet oxygen generator (SOG) motivated many investigations into an electrically driven oxygen-iodine laser (ElectricOIL) that was demonstrated by Carroll *et al.*<sup>2,3</sup> in a supersonic flow cavity. Subsequent efforts have demonstrated gain<sup>4-6</sup> and lasing<sup>5-7</sup> in other ElectricOIL configurations since the earlier demonstrations. For an excellent and comprehensive topical review of discharge production of  $O_2(a)$  and ElectricOIL studies see Ionin *et al.*<sup>8</sup> The demonstrations of ElectricOIL systems raise the possibility of other potential gas mixtures that can be electrically excited and transfer their energy to the iodine atom for subsequent lasing. One option is the use of air because the operational logistics are potentially easier than with  $O_2$ .

In this work, we report on the demonstration of gain and a continuous wave (cw) laser on the  $I^* \rightarrow I$  electronic transition of the iodine atom at 1315 nm pumped by resonance excitation transfer from  $O_2(a)$  produced in an electric discharge sustained in a dry air-He-NO gas mixture. The interest in air discharges stems from logistics considerations, however substantial inert gas dilution is still required to produce the electron energy distributions sufficient to generate satisfactory  $O_2(a)$  yields. If excited states of  $N_2$  and/or N contribute to  $I^*$  excitation, then addition of  $N_2$  to the discharge mixture could be beneficial.

Electric discharge stability and temperature control were found to be critical parameters to obtaining positive gain. Electric discharges sustained in moderate pressures (5-15 of Torr) of oxygen are prone to arcing and constriction. The production of excited oxygen and nitrogen species by the discharge adds higher levels of complexity to the downstream kinetics when the iodine donor species are added to the flow. (These species are not usually encountered in the purely chemical system). The critical aspect of temperature control results from the equilibrium of the singlet delta pumping reaction,

---

\*[carroll@cuaerospace.com](mailto:carroll@cuaerospace.com); phone 1 217 333-8274; fax 1 217 333-4726; [cuaerospace.com](http://cuaerospace.com)



where the forward rate coefficient is  $7.8 \times 10^{-11} \text{ cm}^3/\text{molecule-s}$ ,<sup>9</sup> and the backward rate coefficient is  $1.04 \times 10^{-10} \exp(-403/T) \text{ cm}^3/\text{molecule-s}$ .<sup>10</sup> The equilibrium rate constant ratio of the forward to backward reactions is  $K_{\text{eq}}=0.75 \exp(403/T)$ , where  $T$  is the gas temperature. The yield of  $\text{O}_2(a)$  for optical transparency as a function of temperature is  $Y_{\text{OT}}=1/[1+1.5 \exp(403/T)]$ .<sup>11</sup> Note that the backward rate is slower,  $K_{\text{eq}}$  larger, and  $Y_{\text{OT}}$  lower as  $T$  is decreased.

## 2. DISCHARGE EXPERIMENTS

Three different discharge types were utilized during this work, radio frequency (RF) discharges, pulser-sustainer (P-S) discharges, and microwave discharges. Only the RF and microwave experiments were successful in obtaining conditions sufficient for gain and lasing.

### 2.1 RF and P-S experimental setup

A block diagram of the flow tube setup is shown in Fig. 1. The plasma zone was approximately 4.9 cm in diameter and 25 cm long. For the RF experiments an ENI OEM-25A provided the power for the experiments at 13.56 MHz, and the incident and reflected powers to the RF matching network were measured by a Bird ThruLine model 43 wattmeter (RF “Power” is the difference of the incident and reflected powers). Matching the power to the discharge was achieved using a traditional PI-matching network. For the P-S experiments a specialized pulse circuit<sup>12</sup> with a DC sustainer was used (described in more detail below). In these P-S experiments, the discharge consisted of two hollow cathode electrodes separated by 25 cm which served as the electrodes for the sustainer. A third electrode for the high voltage pulse was added between the hollow cathodes in the form of a capacitive band around the flow tube. The pulser used the same ground as the DC sustainer.

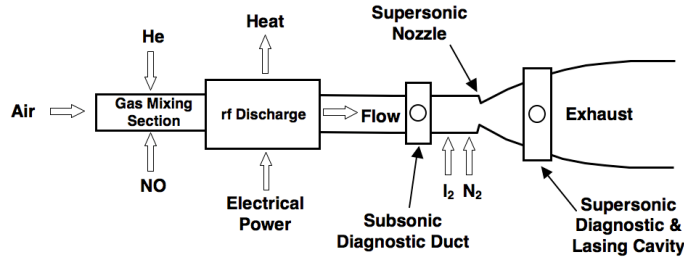


Fig. 1. Schematic of the experimental apparatus.

The subsonic diagnostic duct has four windows through which simultaneous measurements are made of the optical emissions. A Princeton Instruments/Acton Optical Multi-channel Analyzer (OMA-V, 1024-element InGaAs array) with a 0.3 m monochromator and a 600 g/mm grating blazed at  $1 \mu\text{m}$  was used for measurements of  $\text{O}_2(a)$  emission at 1268 nm. Measurements of the  $\text{O}_2(a)$  yield (defined as  $[\text{O}_2(a)]/[\text{O}_2]_{\text{input}}(T,p)$ , where  $[\text{O}_2]_{\text{input}}(T,p)$  is the total input  $\text{O}_2$  density evaluated at the local measured temperature  $T$  and pressure  $p$ ) were obtained from OMA-V calibrations to more complex calibrations involving gain measurements and the relative values of the spectral intensities measured for  $\text{I}^*$  to  $\text{O}_2(a)$  using techniques originally developed by Hager,<sup>13</sup> Davis and Rawlins.<sup>14</sup> This approach provides a lower bound to the  $\text{O}_2(a)$  yields. An Apogee E47 CCD camera coupled to a Roper Scientific/Acton Research 150-mm monochromator was used to measure the emission of  $\text{O}_2(b^1\Sigma)$  at 762 nm to determine flow temperature. The broadband emission of  $\text{NO}_2^*$  was measured using a Hamamatsu R955 photomultiplier with a narrowband 580 nm filter and a 50 mm focal length collection lens; the O-atom concentration was determined from  $\text{NO}_2^*$  using the method described by Piper.<sup>15</sup> These optical diagnostics were fiber coupled using either Oriel model #77538 glass fiber bundles or ThorLabs  $600 \mu\text{m} \times 5 \text{ m}$  multimode fibers. Micro-Motion CMF and Omega FMA mass flow meters were used to measure the flow rates of the gases. Throughout these experiments, “air” was created using a 4:1 mixture of nitrogen to oxygen. Pressures in the flow tubes were measured with MKS Instruments and Leybold capacitance manometers.

### 2.2 RF and P-S discharge experiments

A series of experiments focusing on the production of  $\text{O}_2(a)$  from air was performed using a P-S discharge. Figure 2 shows the results from two tests with the P-S. The addition of helium equal to the amount nitrogen in the air provided an improvement in  $\text{O}_2(a)$  yield although the yield is quite low. In order to directly compare the results from the P-S to the RF discharge, another set of experiments was performed using the hollow cathode electrodes for the RF discharge. The

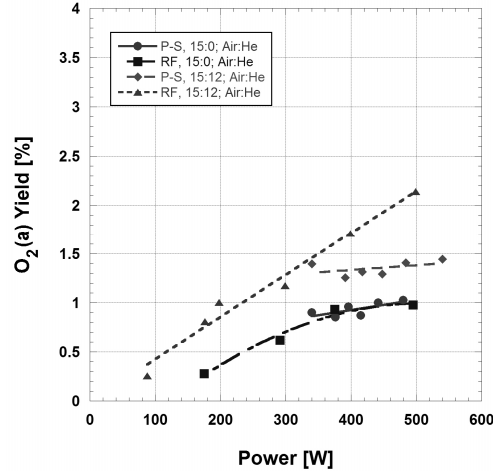


Fig. 2.  $O_2(a)$  Yield vs. Power for the pulser-sustainer (P-S) and radio frequency (RF) discharges using hollow cathode electrodes at 12.5 Torr.

capacitive band was removed during these tests. The results are also shown in Fig. 2. With no helium diluent, the results are similarly poor for both the P-S and the RF discharges, but with even a small amount of helium added to the flow, the RF discharge produced more  $O_2(a)$  and had a more promising slope of  $O_2(a)$  yield versus input power. Other experiments<sup>16</sup> using the P-S were also discouraging, so the efforts with the P-S discharge were discontinued and we focused on the RF and microwave systems.

As Fig. 2 indicates, helium diluent and the RF discharge both improved the  $O_2(a)$  yield for a given power input, so data was collected varying these two parameters. Figure 3 shows the results. A constant NO flow of 0.15 mmol/s was added to each case in Fig. 3, and the discharge was operated with the hollow cathode configuration at 12.5 Torr. The discharge production of  $O_2(a)$  was enhanced by the addition of this small proportion of NO to lower the ionization threshold of the gas mixture. The NO also significantly reduces the concentration of atomic oxygen which has been shown to quench the desired  $I^*$  state.<sup>17,18</sup> The  $O_2(a)$  yield improved dramatically as the helium diluent flow increased.

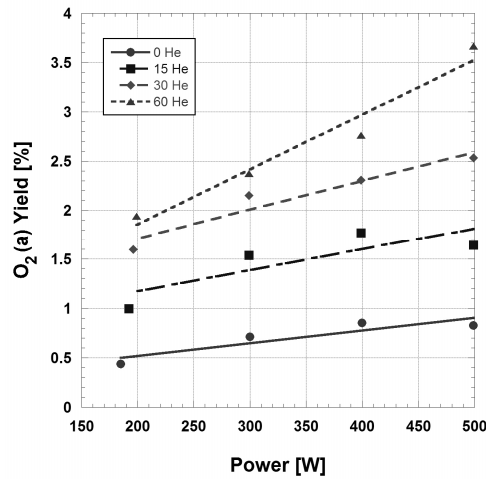


Fig. 3.  $O_2(a)$  Yield vs. Power for the RF discharge using hollow cathode electrodes with constant air and NO flows of 15 and 0.15 mmol/s, respectively at 12.5 Torr with various helium diluent flow rates.

Operating at the low discharge pressure of 12.5 Torr is not desirable for laser operation, so a subsequent set of experiments was performed in which the input power was held constant at 700 Watts while the pressure in the discharge was varied over a wide range. Previous experiments with oxygen and helium discharges have shown that the hollow cathode discharge is not ideal for operation at high pressure.<sup>19</sup>

The data in Fig. 4 and the rest of the data in this section comes from a clamshell RF discharge around a 2 inch diameter flow tube. More information on the performance of this transverse electric discharge sustained in an O<sub>2</sub>-He-NO gas mixture can be found in Zimmerman *et al.* and Woodard *et al.*<sup>20,21</sup> In both cases of 1:1 Air:He (with and without NO), the yield eventually drops as the pressure increases, but in the 1:4 Air:He case, the yield has a peak at about 20 Torr and does not fall too sharply until the pressure is higher than 60 Torr. Figure 5 shows the O<sub>2</sub>(a) yield as a function of total flow rate. Two diluent ratios, 1:1 and 1:4 Air:He are shown, and the power, NO flow rate, and pressure were held constant at 700 W, 0.15 mmol/s, and 20 Torr respectively.

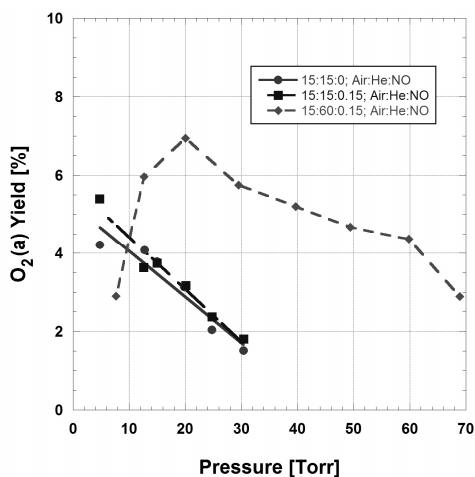


Fig. 4. O<sub>2</sub>(a) Yield vs. Pressure using a clamshell RF discharge at 700 W.

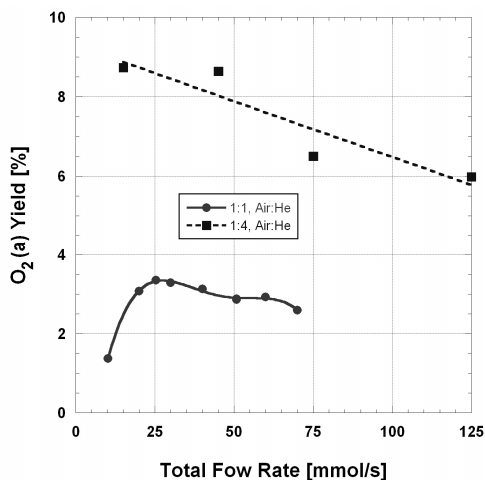


Fig. 5. O<sub>2</sub>(a) Yield vs. Flow Rate with constant discharge power of 700 W, NO flow rate of 0.15 mmol/s, and pressure of 20 Torr.

These data suggested that the RF power input needed to be increased in order to maximize the O<sub>2</sub>(a) yield under conditions having a ratio of helium to air of 4:1 or higher. As such, measurements were made of the O<sub>2</sub>(a) yield and oxygen atom yield as a function of input RF power for a 4:1 helium to air mixture ratio, Fig. 6. The flow of oxygen in this test is 3 mmol/s, and the yield may still be increasing after 1600 W of input power. This finding, compared to data collected with only oxygen and helium, indicates that a large amount of the power is going somewhere other than the oxygen such as excited nitrogen states. As noted above there are many more excited species in this gas discharge with air in the mixture due to the presence of N<sub>2</sub>. It is important to note that there is a strong N<sub>2</sub>(B→A) band around 1220 nm (see below) that grows significantly in strength as the discharge power is increased. At very high powers this N<sub>2</sub>(B→A) spectrum overwhelms the O<sub>2</sub>(a) spectrum thereby making it progressively more difficult to analyze the O<sub>2</sub>(a) yield data. Interestingly, we typically measure gas temperatures that are significantly higher (as much as 50-100 K) with O<sub>2</sub>-He gas discharges than with these air-He discharge gas mixtures; this is another clear indication that large amounts of power are

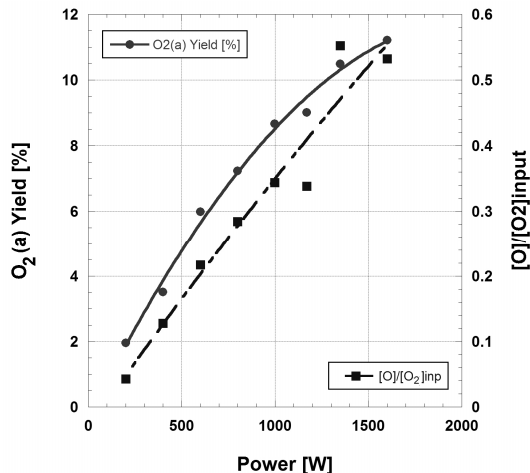


Fig. 6. O<sub>2</sub>(a) Yield and Oxygen Atom Yield vs. Power for 15:60:0.1 mmol/s of Air:He:NO at 20 Torr. Oxygen atom yield is defined as  $[O]/[O_2]_{\text{input}}(T,p)$ , where  $[O_2]_{\text{input}}(T,p)$  is the total input O<sub>2</sub> density evaluated at the local measured temperature T and pressure p.

being absorbed and retained by excited N<sub>2</sub> states, i.e. the energy is not being thermalized as heat into the flow. The O<sub>2</sub>(a) yield and oxygen atom measurements from this test were sufficiently encouraging to introduce iodine into the system.

### 2.3 Subsonic microwave discharge flow reactor experiments

To provide a basis for comparison to O<sub>2</sub>/He discharge systems, we conducted a series of experiments in a subsonic, low-power discharge-flow reactor at low pressures and room temperature. The apparatus is described in detail elsewhere.<sup>4,22-24</sup> It consists of a 5-cm (i.d.) flow reactor with a 2450 MHz, 100 W resonant-cavity microwave discharge and a movable I<sub>2</sub> injector. Typical experimental conditions were 1.5 Torr and 2 mmole/s total flow rate, resulting in flow velocities of ~1250 cm/s. Several optical diagnostics were used to determine the concentrations of the key atomic and molecular species: [O<sub>2</sub>(a)] and [I\*] by near-IR emission spectroscopy, calibrated by a blackbody reference standard; small-signal gain and the quantity  $[I^*]-[I]/2$  by tunable diode laser absorption/gain spectroscopy; and [O] by absolutely calibrated air-afterglow photometry. This apparatus was used to briefly survey the kinetics of O<sub>2</sub>(a) and O production from air/He discharges, for various mole fractions of air (separately mixed as 20%O<sub>2</sub> + 80% N<sub>2</sub>) and also for different O<sub>2</sub>/N<sub>2</sub> ratios.

The discharged air mixtures generated a pronounced green air-afterglow emission along the length of the flow tube, due to the two-body recombination  $O + NO \rightarrow NO_2^* \rightarrow NO_2 + hv$ . NO is produced by the discharge via electron-impact dissociation of N<sub>2</sub>, followed by excitation of ground-state N(<sup>4</sup>S) atoms to the metastable N(<sup>2</sup>D) and the reaction  $N(<sup>2</sup>D) + O_2 \rightarrow NO + O$ .<sup>25</sup> For certain limited ranges of conditions, we also observed near-IR chemiluminescence from atom recombination in the flow tube as shown in Figs. 7 and 8. At the lower air mole fractions, we observed the spectrum shown in Fig. 7. The band centered near 1270 nm is the familiar O<sub>2</sub>(a<sup>1</sup>Δ→X<sup>3</sup>Σ) emission, and the prominent band centered at 1224 nm is the (0,0) band of the NO(C<sup>2</sup>Π→A<sup>2</sup>Σ<sup>+</sup>) transition. The NO(C) state is formed directly by the two-body recombination reaction  $N + O \rightarrow NO(C)$ , which proceeds directly into the v=0 level via inverse predissociation.<sup>26</sup> NO(C) has a very short radiative lifetime, ~50 ns, and is thus present at concentrations on the order of 10<sup>3-4</sup> cm<sup>-3</sup> compared to O<sub>2</sub>(a) and O concentrations of 10<sup>14-15</sup> cm<sup>-3</sup>. The accompanying UV band systems of NO(C<sup>2</sup>Π→X<sup>2</sup>Π, A<sup>2</sup>Σ<sup>+</sup>→X<sup>2</sup>Π) are undoubtedly also present, although we have not attempted to observe them. Note that the intensities of these features are related not to the amount of ground-state NO present, but rather to the product of the ground-state N and O concentrations. We also observed N<sub>2</sub>(B<sup>3</sup>Π<sub>g</sub>→A<sup>3</sup>Σ<sub>u</sub><sup>+</sup>) emission arising from three-body recombination of N atoms. Figure 8 shows the (0,0) band of this system at ~1030-1050 nm. At reduced O<sub>2</sub>/N<sub>2</sub> ratios we have also observed the (0,1) band near 1220-1240 nm. Numerous vibrational levels of the B-state are populated by this process, giving rise to B→A emission in bands throughout the visible and near-IR, known as the Nitrogen First Positive or Lewis-Rayleigh afterglow. The N<sub>2</sub>(B) state also has a short radiative lifetime, ~6 μs, so is present at concentrations <10<sup>6</sup> cm<sup>-3</sup>. Addition of NO eliminates the NO(C) and N<sub>2</sub>(B) emissions via removal of N atoms:  $N + NO \rightarrow N_2 + O$ .

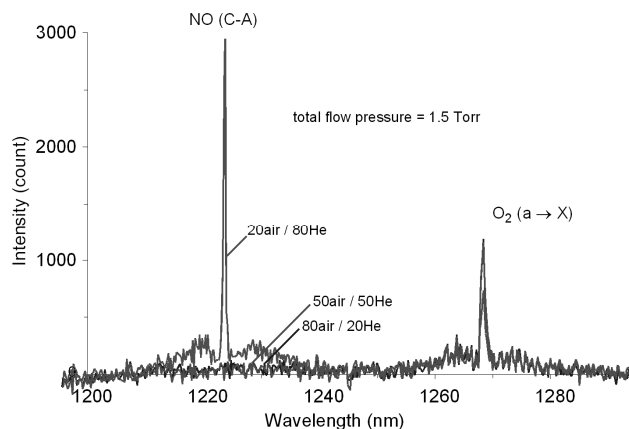


Fig. 7. Spectra of NO(C→A) and O<sub>2</sub>(a→X) emission observed at 1.5 Torr and 70 W discharge power.

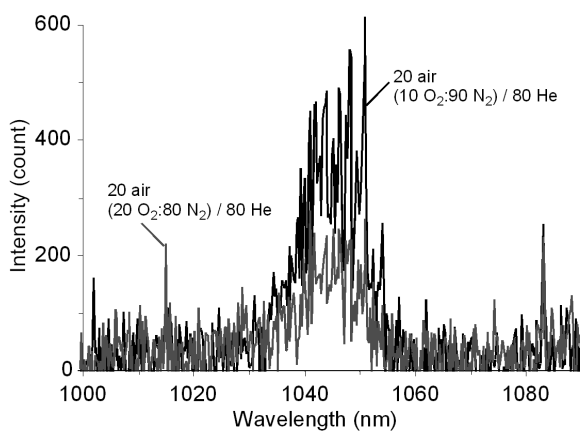


Fig. 8. Spectra of the (0,0) band of the N<sub>2</sub>(B→A) emission observed at 1.5 Torr and 70 W discharge power.

We determined the dependence of the O<sub>2</sub>(a) yield on the air mole fraction in air(20%O<sub>2</sub>+80%N<sub>2</sub>)/He mixtures, for comparison to similar measurements with O<sub>2</sub>/He mixtures. Yields for 1.5 Torr and 2 mmole/s are shown in Fig. 9. The O<sub>2</sub>(a) yields, defined as [O<sub>2</sub>(a)]/[O<sub>2</sub>]<sub>0</sub>, for a given air mole fraction are the same as we observe for that mole fraction of O<sub>2</sub>, i.e. the fraction of O<sub>2</sub> that is excited to O<sub>2</sub>(a) by the discharge depends only on the mole fraction of total diatomic species (for a given pressure and flow velocity). The yields increase with decreasing diatomic mole fraction as the electron energy distribution becomes more energetic, promoting increased ionization and electron-impact excitation rates.<sup>22,27</sup>

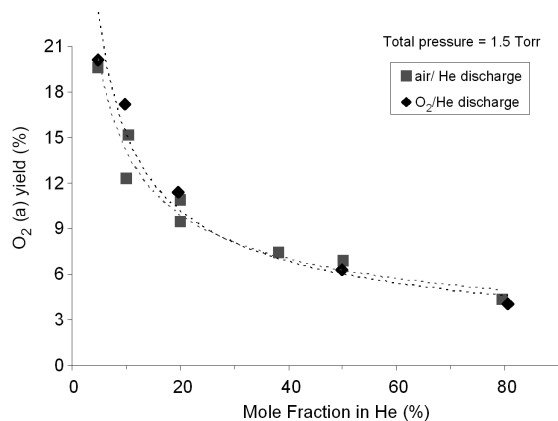


Fig. 9. O<sub>2</sub>(a) yields observed for air/He and O<sub>2</sub>/He mixtures, 1.5 Torr, 70 W discharge power.

We observed the reaction of the air/He discharge effluents with  $I_2$  to excite  $I^*$ . The experiments produced low  $[I^*]/[I]$  ratios and net  $I \rightarrow I^*$  absorption, in keeping with previous room-temperature results for  $O_2/Ar$  discharges (without  $NO_2$  addition).<sup>4,22,23</sup> We also investigated the excitation of  $I^*$  for  $N_2/He$  discharges. For 6% and 20%  $N_2/He$  at 1.0 and 1.5 Torr, flow velocities of 1000 to 1600 cm/s, we observed  $I^*$  emission signals which were about 100 times less intense than observed for  $O_2/Ar$  and  $O_2/He$  discharges under similar conditions. This low  $I^*$  excitation rate may be due to the relatively low concentrations of reactive and excited-state species in the  $N_2$  discharge effluent. Thus, while  $N_2$  discharge effluents do indeed dissociate  $I_2$  and excite  $I^*$ , the reaction provides a negligible contribution to  $I^*$  excitation by  $O_2$  discharge products. From the low-power, room-temperature results, it appears that the participation of  $N_2$  in  $O_2(a)$  and  $I^*$  excitation is primarily that of a largely inactive diatomic diluent.

### 3. GAIN AND LASING EXPERIMENTS

#### 3.1 RF-driven reactor

The supersonic diagnostic cavity, Fig. 1, has a Mach 2 nozzle with windows that serve as view ports. Measurements of gain (or absorption) were made prior to running the apparatus as a laser using the Iodine-Scan Diagnostic (ISD) developed by Davis and co-workers.<sup>28</sup> The ISD is a diode laser based monitor for the small signal gain in iodine lasers. The system uses a single mode, tunable diode laser that is capable of accessing all six hyperfine components of the atomic iodine. It was calibrated in frequency to enable automated operation for the (3,4) hyperfine transition for our experiments. A fiber optic cable was used to deliver the diode laser probe beam to the iodine diagnostic regions in the subsonic portion of the flow tube and in the supersonic cavity. Since the ISD uses a narrow band diode laser, measurements of the lineshapes can also be used to determine the local temperature from the Voigt profile. The windows on the sides of the cavity when using the gain diagnostic were wedged and anti-reflection coated to minimize etalon effects. A single pass configuration (5 cm path length) was used in the supersonic diagnostic section.

Laser power measurements were made with a Scientech Astral™ model AC5000 calorimeter interfaced to a Scientech Vector™ model S310 readout, and were made at the same location in the supersonic laser cavity as the gain measurements. The mirrors were then put in place for the laser power trials. Two mirrors with 2 m radius of curvature, purchased from Advanced Thin Films (ATF), formed a stable optical cavity. Measurements of transmission,  $T$ , indicated a transmission of  $0.003\% \pm 0.001\%$ . Direct measurements of mirror reflectivity,  $R$ , and absorption/scattering,  $AS$ , were unavailable, but previous reflectivity measurements of similar mirrors indicated that a fraction of the remainder of  $1-T$  is in  $AS$  losses for similar high reflectivity mirrors. Thus, we estimate that the mirrors each had a reflectivity of  $99.996\% \pm 0.001\%$ . The mirrors were separated by approximately 34 cm. An Infrared (IR) Detection Card from New Focus, Model 5842, with response between 800-1600 nm, was also used to observe the intensity profile of the beam.

Several flow conditions were found that resulted in positive gain using the RF discharge configuration shown in Fig. 1. A typical set of conditions are 3.0 mmol/s of  $O_2$  mixed with 12.0 mmol/s of  $N_2$  to create approximately 15.0 mmol/s of dry air which is diluted with 75.0 mmol/s of He and 0.1 mmol/s of NO. A secondary stream of  $\approx 0.040$  mmol/s of  $I_2$  with 12.0 mmol/s of secondary He diluent was injected  $\approx 27.3$  cm downstream from the exit of the discharge. A tertiary flow of 155 mmol/s of cold  $N_2$  gas ( $\approx 120$  K) was injected further downstream to lower the temperature and to raise the pressure to improve the performance of the nozzle with our vacuum system. The pressures in the subsonic diagnostic duct and in the supersonic diagnostic cavity were 44.0 Torr and 2.0 Torr, respectively.

BLAZE-IV simulations were performed for these flow conditions and yields and indicated that this magnitude of yield should be sufficient for gain and lasing in our experimental configuration.<sup>29</sup> In order to simulate the performance of the  $O_2-N_2$  discharge component of an electric nitrogen-oxygen-iodine laser device 17 species and 119 reactions were added to the BLAZE-IV model. These computations also indicated lower flow temperatures with  $N_2$  in discharge gas mixture (not shown for brevity).

Gain was then measured for the above flow conditions at 1750 W of RF discharge power and is shown in Fig. 10 with a peak of 0.0062 %/cm at line center. The lineshape indicates a temperature of approximately 180 K. Figure 10 also shows the important effect of NO for this laser system: optical gain occurs with NO in the discharge gas mixture, but only optical absorption is present when NO is removed from the mixture. Figure 11 shows the gain as a function of RF power. Interestingly, as the RF power is reduced below approximately 900 W only optical transparency is observed rather than absorption. We believe this phenomenon is due to a lack of molecular iodine dissociation (and hence little or no atomic iodine) at this point due to O atoms being reduced by both the presence of NO through a cyclic recombination<sup>30</sup> and

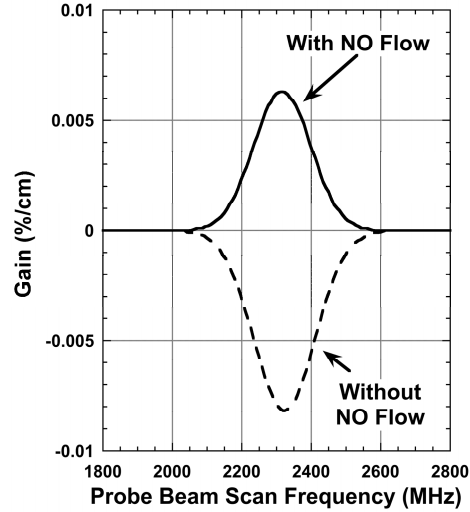


Fig. 10. Gain lineshape in the supersonic cavity as a function of probe beam scan frequency with and without NO in the discharge gas mixture. Discharge power was 1500 W.

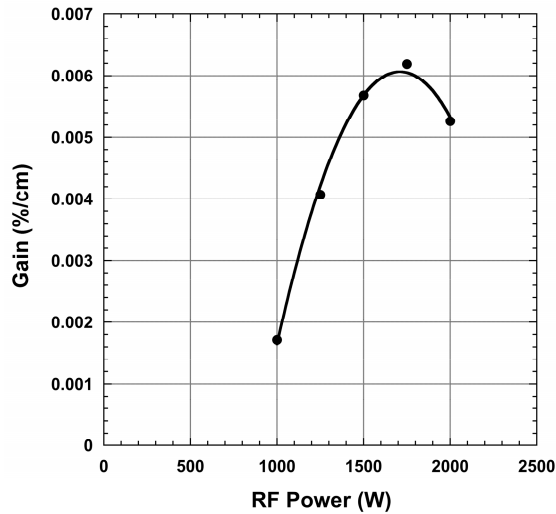


Fig. 11. Gain in the supersonic cavity as a function of RF discharge power.

through three-body recombination of O atoms at the higher pressure of 45 Torr for these cases. This hypothesis is supported by Fig. 10 which shows absorption when the NO was removed from the discharge gas mixture.

The laser resonator was subsequently installed around the supersonic cavity. For the above flow conditions and 1500 W RF power, a laser output power of 32 mW was obtained. The beam shape was a rounded rectangle with a length of  $\approx 1.9$  cm (the same as the clear aperture of the mirror mounts) and a height of  $\approx 1.1$  cm. For reference, the initial measurement of laser action using an electrically driven oxygen-iodine laser with a supersonic laser cavity at  $\approx 1.3$  Torr produced 220 mW.<sup>3</sup>

### 3.2 Microwave-driven reactor

Gain and lasing measurements were performed in the microwave-driven supersonic flow reactor shown in Fig. 12. The apparatus is described in more detail by Davis et al.<sup>7</sup>  $O_2/N_2$  or  $O_2$  alone, mixed with helium and a small amount of added NO, were excited by a 2450 MHz coaxial discharge at 1 kW power, and passed through a 5-cm-wide rectangular flow duct, Mach  $\sim 2$  nozzle, and supersonic cavity as shown in the figure.  $I_2$  vapor was injected into the subsonic flow 8 cm ( $\sim 1$  ms flow time) upstream of the nozzle throat. Total flow rates were 40-80 mmole/s, resulting in subsonic flow pressures of 20-50 Torr. Discharge E/N values ranged from 20 to 50 Td. Concentrations of  $O_2(a)$ ,  $I^*$ ,  $I$ , and  $O$ , and small-signal gains, were determined by the optical diagnostics listed above in Subsection 2.3.

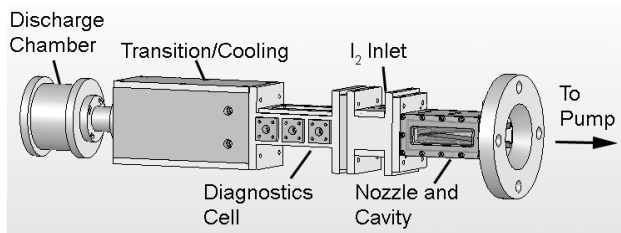


Fig. 12. Microwave-driven supersonic flow reactor.

Typical small-signal gain results are shown in Fig. 13, for different flow rates of NO admitted to the discharge. The measurements were made for 9% air/He at 49 mmole/s, and an injected  $I_2$  flow rate of  $4.7 \mu\text{mole/s}$ . The supersonic flow temperature sampled by the gain measurements was 160 K. In the absence of added NO, the signal shows net absorption, i.e. the NO produced by the discharge is not sufficient to offset  $O + I^*$  quenching. As NO is added, the absorption decreases and eventually positive gain is observed. The variations of  $[I^*]/[I]$  and  $O_2(a)$  yield with added NO are illustrated in Fig. 14. The 9% air/He results are compared to measurements at similar flow conditions for 5%  $O_2/He$ . The  $O_2(a)$  yields increase slightly with added NO, as has been noted previously.<sup>24,30</sup> Note that the  $O_2(a)$  yields for 9% air/He are lower than those for 5%  $O_2/He$  in accord with the diatomic gas mole fraction effect shown in Fig. 9. In both cases, the optimum gain is observed at  $\sim 0.4$  mmole/s NO, indicating similar O concentrations for the two cases. In support of this conclusion, quantitative air-afterglow measurements indicated similar initial O yields of  $\sim 15\%$  for each case, and pronounced exponential decay of O with increasing NO as expected for the O removal reaction sequence:<sup>30</sup>

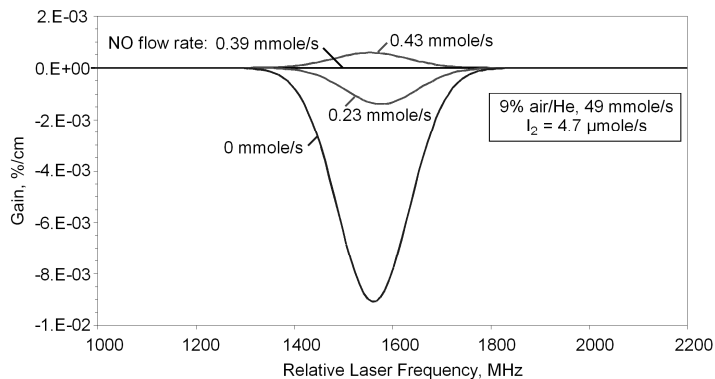


Fig. 13. Gain measurements in microwave-driven air/He supersonic flow, for different NO flow rates admitted to the discharge (1 kW discharge power).

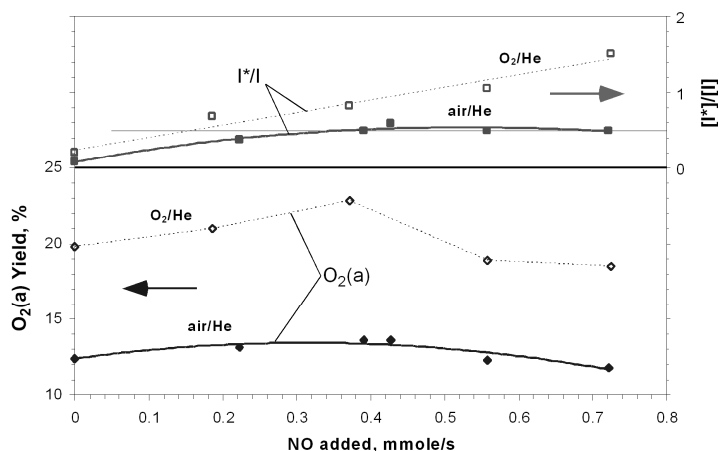


Fig. 14. Effect of added NO on  $[I^*]/[I]$  and  $O_2(a)$ : 1 kW microwave discharge power, 9% air/He and 4.9%  $O_2/He$ , 49 mmole/s.



The inversion ratio,  $[\text{I}^*]/[\text{I}]$ , for the air/He case passes through a maximum and remains near threshold with increasing NO. This behavior is in marked contrast to that for  $\text{O}_2/\text{He}$ , where  $[\text{I}^*]/[\text{I}]$  continues to increase with increasing NO even though the gain is decreasing due to reduced  $\text{I}_2$  dissociation.<sup>7</sup> This differing behavior suggests the possibility of somewhat different  $\text{I}^*$  production and quenching mechanisms for the two mixtures. Note that, based on Reaction (1), the “equilibrium”  $[\text{I}^*]/[\text{I}]$  values at 160 K corresponding to the observed  $\text{O}_2(\text{a})$  yields at maximum gain are  $\sim 1.5$  for the air/He case and  $\sim 2.7$  for the  $\text{O}_2/\text{He}$  case. The observed  $[\text{I}^*]/[\text{I}]$  values are well below the equilibrium for Reaction (1), even with suppressed  $\text{O} + \text{I}^*$  quenching.

Laser power extraction measurements were made using a stable resonator assembly with two 1-inch diameter mirrors, each with 99.997% reflectivity, centered in the supersonic flow 4.35 cm downstream of the nozzle throat. The output power was observed with power meters on each side of the resonator assembly, with a 5-cm gain length. The total flow rates were  $\sim 70$  to 80 mmole/s, with  $\text{I}_2$  flow rates of  $\sim 20$   $\mu\text{mole/s}$ . The mixtures did not lase for the  $\text{O}_2/\text{N}_2$  ratio of air, so we increased the  $\text{O}_2/\text{N}_2$  ratio until lasing could be observed. The dependence of output power on  $\text{O}_2/\text{N}_2$  ratio is shown in Fig. 15, for 5% and 9.5% ( $\text{O}_2+\text{N}_2$ ) in He. The power increases linearly with increasing  $\text{O}_2$  fraction, consistent with the behavior of  $\text{N}_2$  as a chemically inactive diluent as noted above. Note that the extracted powers are much smaller than the  $\text{O}_2(\text{a})$  power above threshold in these flows (e.g. 27 W above threshold for the 5%  $\text{O}_2/\text{He}$  case at 82 mmole/s). This is due primarily to the inherent inefficiency of the high-reflectivity, small-diameter resonator used in these measurements,<sup>7</sup> and to a lesser extent to non-equilibrium  $\text{I}^*$  losses in the reacting flow.<sup>22</sup>

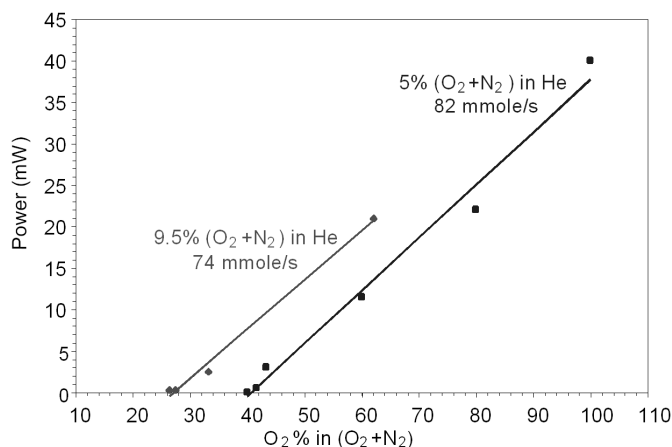


Fig. 15. Laser power extracted: 1 kW microwave discharge of  $\text{O}_2/\text{N}_2/\text{He}/\text{NO}$  mixtures, 5% and 9.5% ( $\text{O}_2+\text{N}_2$ ) in He.

#### 4. CONCLUSIONS

In conclusion, gain and cw laser action were measured on the  $\text{I}^* \rightarrow \text{I}$  electronic transition of the iodine atom at 1315 nm pumped by a near resonant energy transfer from  $\text{O}_2(\text{a})$  produced in an electric discharge sustained in dry  $\text{O}_2\text{-N}_2\text{-He-NO}$  gas mixtures. Comparable results were achieved with both RF and microwave sources, however a non-self-sustained pulser-sustainer source generated insufficient  $\text{O}_2(\text{a})$  yields. Several highly energetic excited states of  $\text{N}_2$  and NO are produced in these discharge gas mixtures in addition to  $\text{O}_2(\text{a})$ . It is possible that some of these states can influence the production/destruction of  $\text{I}^*$ , however our results to date show that this is not the case for the range of flow conditions we have sampled. These excited states tend to be highly labile, short-lived, and present at relatively low concentrations for the discharge effluent conditions we have used here. Further investigation at fast flow velocities and low pressures is required to examine the effects of these states more directly.

In the RF-driven reactor, cold  $\text{N}_2$  was injected to lower the temperature of the flow and shift the equilibrium of atomic iodine in favor of the  $\text{I}^*$  state. This effect, in combination with a supersonic flow cavity, produced sufficient population inversion to observe gain of 0.0062 %/cm, followed by laser oscillations when two  $\sim 99.996\%$  reflectivity mirrors were

used to form an optical resonator surrounding the gain medium. The laser output power for these experimental conditions was 32 mW.

In subsonic and supersonic microwave-driven reactors, we observed  $O_2(a)$  yields for a given air mole fraction which were the same as those observed for the equivalent mole fraction of  $O_2$  in  $O_2/He$  mixtures. We also observed concomitantly less  $I^*$  excitation for the air/He case, and possibly increased  $I^*$  loss as well. Although  $N_2$  discharge products were observed to give a small degree of  $I^*$  excitation, the primary role of  $N_2$  in the air/He discharge system appears to be as a largely unreactive diluent in both the  $O_2(a)$  production and the  $I^*$  excitation/deactivation chemistry. Thus the use of air instead of  $O_2$  as the feedstock for an EOIL system would require operation at significantly higher pressures and flow rates to make up for the  $N_2$  dilution effects. Potential operational logistics make the use of air rather than  $O_2$  an interesting option, but the tradeoffs in efficiency and performance need to be carefully assessed.

### ACKNOWLEDGEMENTS

This work was supported by DARPA contract HR0011-07-C-0054. The authors gratefully thank D.M. King, J.K. Laystrom, A. Roberts, D.B. Oakes, J. Haney, and D. Vu for their technical assistance.

### REFERENCES

- [1] McDermott, W., Pchelkin, N., Benard, D., and Bousek, R., "An electronic transition chemical laser," *Appl. Phys. Lett.* 32(8), 469 (1978).
- [2] Carroll, D. L., Verdeyen, J. T., King, D. M., Zimmerman, J. W., Laystrom, J. K., Woodard, B. S., Richardson, N., Kittell, K., Kushner M. J. and Solomon, W. C., "Measurement of positive gain on the 1315 nm transition of atomic iodine pumped by  $O_2(a^1\Delta)$  produced in an electric discharge," *Appl. Phys. Lett.* 85(8), 1320 (2004).
- [3] Carroll, D. L., Verdeyen, J. T., King, D. M., Zimmerman, J. W., Laystrom, J. K., Woodard, B. S., Benavides, G. F., Kittell, K., Stafford, D. S., Kushner, M. J., and Solomon, W. C., "Continuous-wave laser oscillation on the 1315 nm transition of atomic iodine pumped  $O_2(a^1\Delta)$  produced in an electric discharge," *Appl. Phys. Lett.* 86, 111104 (2005).
- [4] Rawlins, W. T., Lee, S., Kessler, W. J. and Davis, S. J., "Observations of gain on the  $I(^2P_{1/2}^2P_{3/2})$  transition by energy transfer from  $O_2(a^1\Delta_g)$  generated by a microwave discharge in a subsonic-flow reactor," *Appl. Phys. Lett.* 86, 051105 (2005).
- [5] Verdeyen, J. T., Carroll, D. L., King, D. M., Laystrom, J. K., Benavides, G. F., Zimmerman, J. W., Woodard, B. S. and Solomon, W. C., "Continuous-wave laser oscillation in subsonic flow on the 1315 nm atomic iodine transition pumped by electric discharge produced  $O_2(a^1\Delta)$ ," *Appl. Phys. Lett.* 89, 101115 (2006).
- [6] Hicks, A., Tirupathi, S., Jiang, N., Utkin, Y., Lempert, W. R., Rich, J. W., and Adamovich, I. V., "Design and operation of a supersonic flow cavity for a non-self-sustained electric discharge pumped oxygen-iodine laser," *J. Phys. D: Appl. Phys.* 40, 1408-1415 (2007).
- [7] Davis, S. J., Lee, S., Oakes, D. B., Haney, J., Magill, J. C., Paulsen, D. A., Cataldi, P., Galbally-Kinney, K. L., Vu, D., Pox, J., Kessler, W. J., and Rawlins, W. T., "EOIL Power Scaling in a 1-5 kW Supersonic Discharge-Flow Reactor," *SPIE Vol. 6874, Paper 10* (2008).
- [8] Ionin, A. A., Kochetov, I. V., Napartovich, A. P. and Yuryshv, N. N., "Physics and engineering of singlet delta oxygen production in low-temperature plasma," *J. Phys. D: Appl. Phys.* 40,R25 (2007).
- [9] Derwent, R.G. and Thrush, B. A., "Excitation of iodine by singlet molecular oxygen. Part 2.—Kinetics of the excitation of the iodine atoms," *Discuss. Faraday Soc.*, 53, 162 (1972).
- [10] Perram, G. P. and Hager, G. D., "The Standard COIL Kinetics Package," Final Report AFWL-TR-88-50 (Air Force Weapons Laboratory, Kirtland Air Force Base (1988).
- [11] Hon, J., Hager, G., Helms, C. and Truesdell, K., "A heuristic method for evaluating COIL performance," *AIAA J.*, 34(8), 1595 (1996).
- [12] Verdeyen, J. T., Nee, B. M., and Carroll, D. L., "Pulse Circuit," U.S. Patent No. 2008/0197714 A1, (2008).
- [13] Hager, G. D., (private communication with Rawlins, W. T. and Carroll, D. L.).
- [14] Rawlins, W. T., Davis, S. J., Lee, S., Silva, M. L., Kessler, W. J., and Piper, L. G., "Optical Diagnostics and Kinetics of Discharge-Initiated Oxygen-Iodine Energy Transfer," *AIAA*, 2003-4032 (2003).
- [15] Piper, L. G., Caledonia, G. E., and Kennealy, "Rate constants for deactivation of  $N_2(A^3\Sigma^+, v_i = 0,1)$  by  $O_2$ ," *J. P., J. Chem. Phys.* 75, 2847 (1981).

- [16] Carroll, D. L., Benavides, G. F., Zimmerman, J. W., Woodard, B. S., Palla, A. D., Verdeyen, J. T., and Solomon, W. C., "Systematic development of the electric discharge oxygen-iodine laser," SPIE Proceedings of the XVII International Symposium on Gas and Chemical Lasers and High Power Lasers, to be published (2009).
- [17] Azyazov, V. N., Antonov, I. O., Ruffner, S. and Heaven, M. C., "Quenching of  $I(^2P_{1/2})$  by  $O_3$  and  $O(^3P)$ ," SPIE Vol. 6101, 61011Y (2006).
- [18] Carroll, D. L., Verdeyen, J. T., King, D. M., Zimmerman, J. W., Laystrom, J. K., Woodard, B. S., Benavides, G. F., Kittell, K. and Solomon, W. C., "Path to the measurement of positive gain on the 1315-nm transition of atomic iodine pumped by  $O_2(a^1\Delta)$  produced in an electric discharge," IEEE J. Quant. Elect. 41(2), 213 (2005).
- [19] Benavides, G. F., Zimmerman, J. W., Woodard, B. S., Palla, A. D., Carroll, D. L., Verdeyen, J. T., King, D. M., Laystrom, J. K., Field, T. H., and Solomon, W. C., "Hybrid electric oxygen-iodine laser performance enhancements and measurements," J. of Directed Energy, to be published (2008).
- [20] Zimmerman, J. W., Woodard, B. S., Verdeyen, J. T., Carroll, D. L., Field, T. H. and Solomon, W. C., "Improved production of  $O_2(a^1\Delta)$  in capacitively coupled radio-frequency discharges," Proc. SPIE 6874, 68740C (2008).
- [21] Woodard, B. S., Zimmerman, J. W., Verdeyen, J. T., Carroll, D. L., Field, T. H., Benavides, G. F., Palla, A. D., and Solomon, W. C., "Improved production of  $O_2(a^1\Delta)$  in transverse radio-frequency discharges," Proc. SPIE 7005, 70051L (2008).
- [22] Rawlins, W. T., Lee, S., Kessler, W. J., Piper, L. G., and Davis, S. J., "Advanced diagnostics and kinetics of oxygen-iodine laser systems," AIAA Paper 2005-5299 (2005).
- [23] Rawlins, W. T., Lee, S. and Davis, S. J., "Kinetics of oxygen discharges and  $I(^2P_{1/2})$  excitation for EOIL," SPIE Vol. 6454, Paper 18 (2007)
- [24] Rawlins, W. T., Lee, S. and Davis, S. J., "Production of Metastable Singlet Oxygen in the Reaction of Nitric Oxide with Active Oxygen," SPIE Vol. 6874, Paper 8 (2008).
- [25] Rawlins, W. T., Fraser, M. E. and Miller, S. M., "Rovibrational Excitation of Nitric Oxide in the Reaction of  $O_2$  with Metastable Atomic Nitrogen," J. Phys. Chem. 93, 1097 (1989).
- [26] Kenner R. D. and Ogryzlo, E. A., [Chemi- and Bioluminescence], "Chemiluminescence in Gas Phase Reactions," Burr, J. G. Ed., Marcel Dekker, Inc. New York, 45-185 (1985).
- [27] Rawlins, W. T., Caledonia, G. E. and Armstrong, R. A., "Dynamics of Vibrationally Excited Ozone Formed by Three Body Recombination. II: Kinetics and Mechanism," J. Chem. Phys. 87, 5209 (1987).
- [28] Davis, S. J., Allen, M. G., Kessler, W. J., McManus, K. R., Miller, M. F. and Mulhall, P. A., "Diode Laser Based Sensors for Chemical Oxygen Iodine Lasers," SPIE Vol. 2702, 195 (1996).
- [29] Palla, A. D., Zimmerman, J. W., Woodard, B. S., Carroll, D. L., Verdeyen, J. T., Lim, T. C. and Solomon, W. C., "Oxygen Discharge and Post-Discharge Kinetics Experiments and Modeling for the Electric Oxygen-Iodine Laser System," J. Phys. Chem. A, 111(29), 6713 (2007).
- [30] Zimmerman, J. W., King, D., Palla, A., Verdeyen, J., Carroll, D., Laystrom, J., Benavides, G., Woodard, B., Solomon, W., Rawlins, W., Davis, S. and Heaven, M., "Important kinetic effects in the hybrid ElectricOIL system," SPIE Vol. 6261, 62611R1-12 (2006).